

SUPPLEMENTARY DATA 5

**Unriddling an old dolphin: platanistoid Notocetus vanbenedeni Moreno, 1892 from the
early Miocene of Patagonia (Argentina)**

MARIANA VIGLINO¹, MÓNICA R. BUONO¹, YOSHIHIRO TANAKA², JOSÉ I. CUITIÑO¹
and R. EWAN FORDYCE³

¹Instituto Patagónico de Geología y Paleontología, CCT CONICET-CENPAT, Bvd. Brown
2915, Puerto Madryn, Chubut, U9120ACD, Argentina.

²Osaka Museum of Natural History, Nagai Park 1-23, Higashi-Sumiyoshi-ku, Osaka, 546-0034,
Japan.

³Department of Geology, University of Otago, Box 56, Dunedin, 9054, New Zealand.

Supplementary Data 5. Supplementary figures for the anatomical description of *Notocetus vanbenedeni*, as well as full cladograms. Note that for the analyses under implied weights, only MPTs of K= 6, 9, 14, 18, and 25 are shown, as their topology was different between themselves and with the strict consensus of the analysis under equal weights.



FIGURE S1. Lateral view of the skull of *Notocetus vanbenedeni*, MPEF-PV 2580 (top) and MLP 5-5 holotype (bottom).

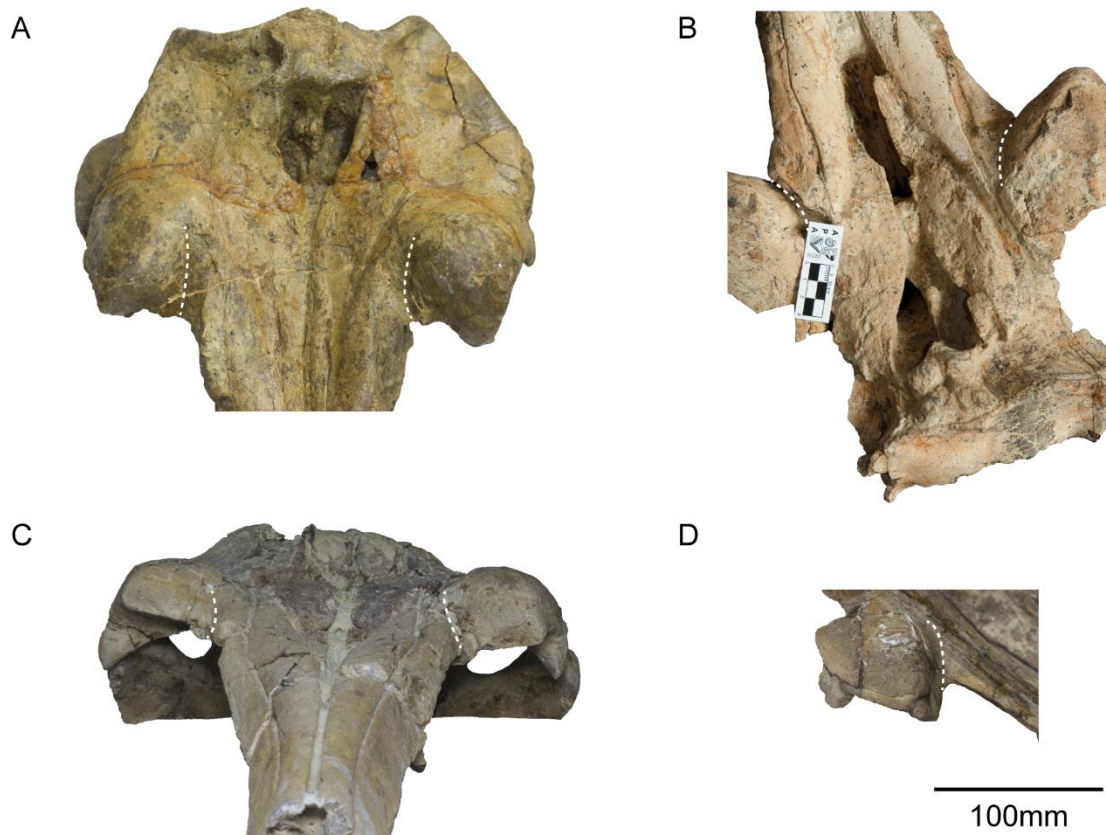


FIGURE S2. Anterior (A, C, D) and dorsal (B) view of *Notocetus vanbenedeni*, showing the wedge posterior to the antorbital notch, between the maxilla at the orbital region and at the rostrum region. **A**, MLP 5-10 (holotype); **B**, MPEF-PV 1660; **C**, MPEF-PV 2580; **D**, MLP 5-10.

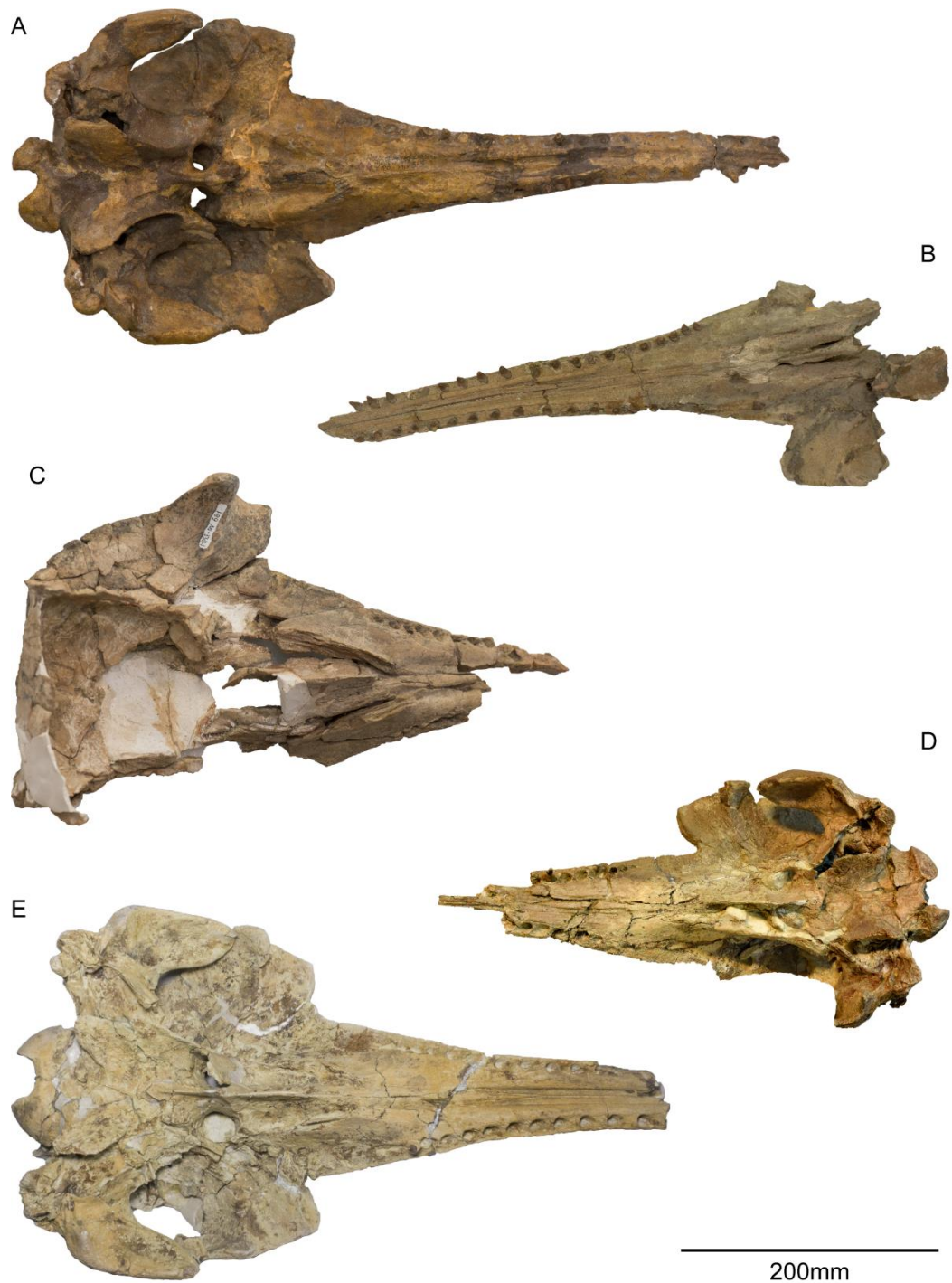


FIGURE S3. Ventral view of *Notocetus vanbenedeni*, showing the orientation of the alveolar groove **A**, MLP 5-10 (holotype); **B**, MLP 5-10; **C**, MPEF-PV 681; **D**, MPEF-PV 1804; **E**, MPEF-PV 2580.

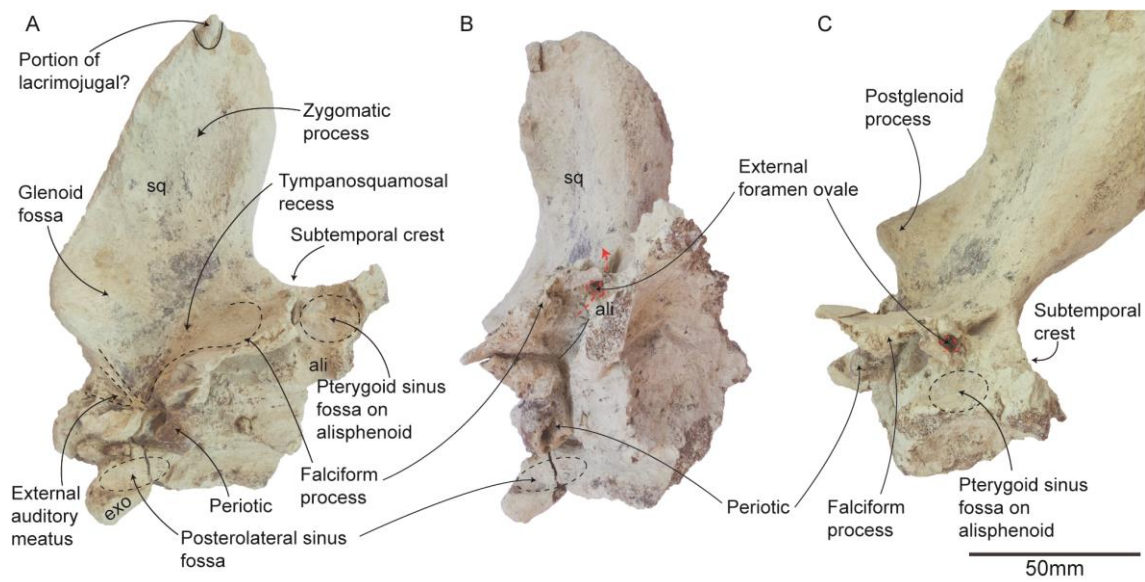


FIGURE S4. Details of the squamosal area in *Notocetus vanbenedeni* with periotic *in situ* (MPEF-PV 2580). Red arrows indicate the position and inferred direction of the external foramen ovale, where the mandibular nerve emerged. Continuous lines indicate sutures, and dashed lines indicate important structures. **A**, ventral; **B**, posteromedial; and **C**, anterior views. **Abbreviations:** **ali**, alisphenoid; **sq**, squamosal; **exo**, exoccipital.

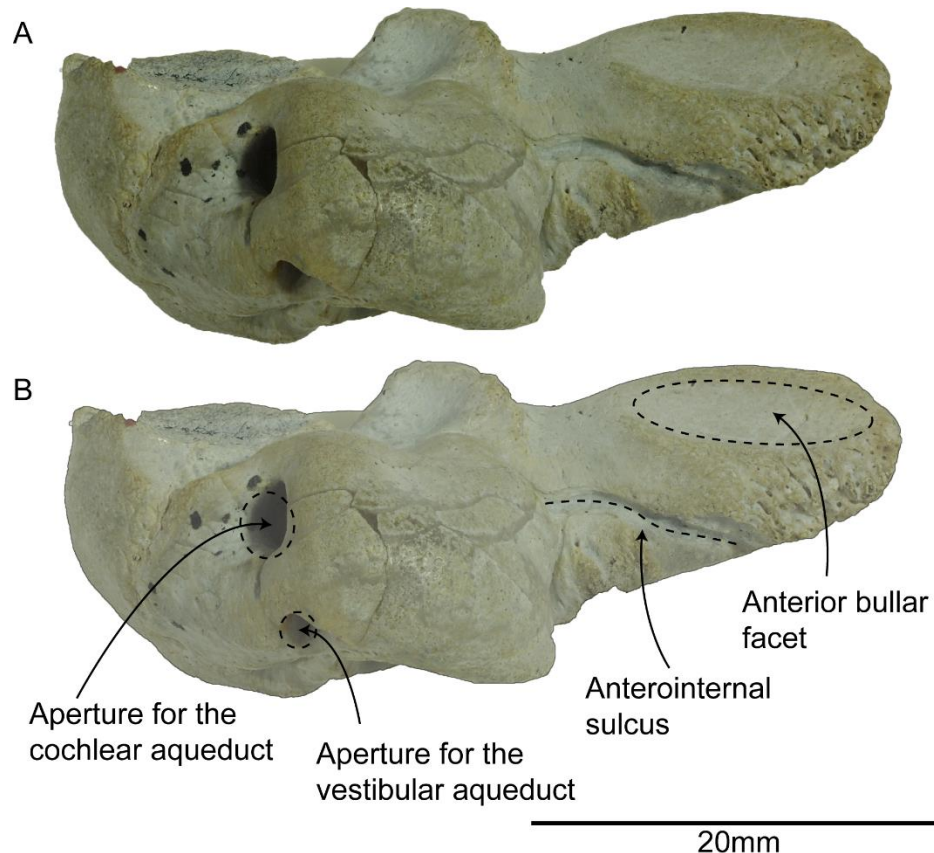


FIGURE S5. Detail of the anterointernal sulcus in the anterior process of the right periotic of *Notocetus vanbenedeni* (MLP 76-IX-2-5). **A**, medial view without labels; **B**, medial view with labels.

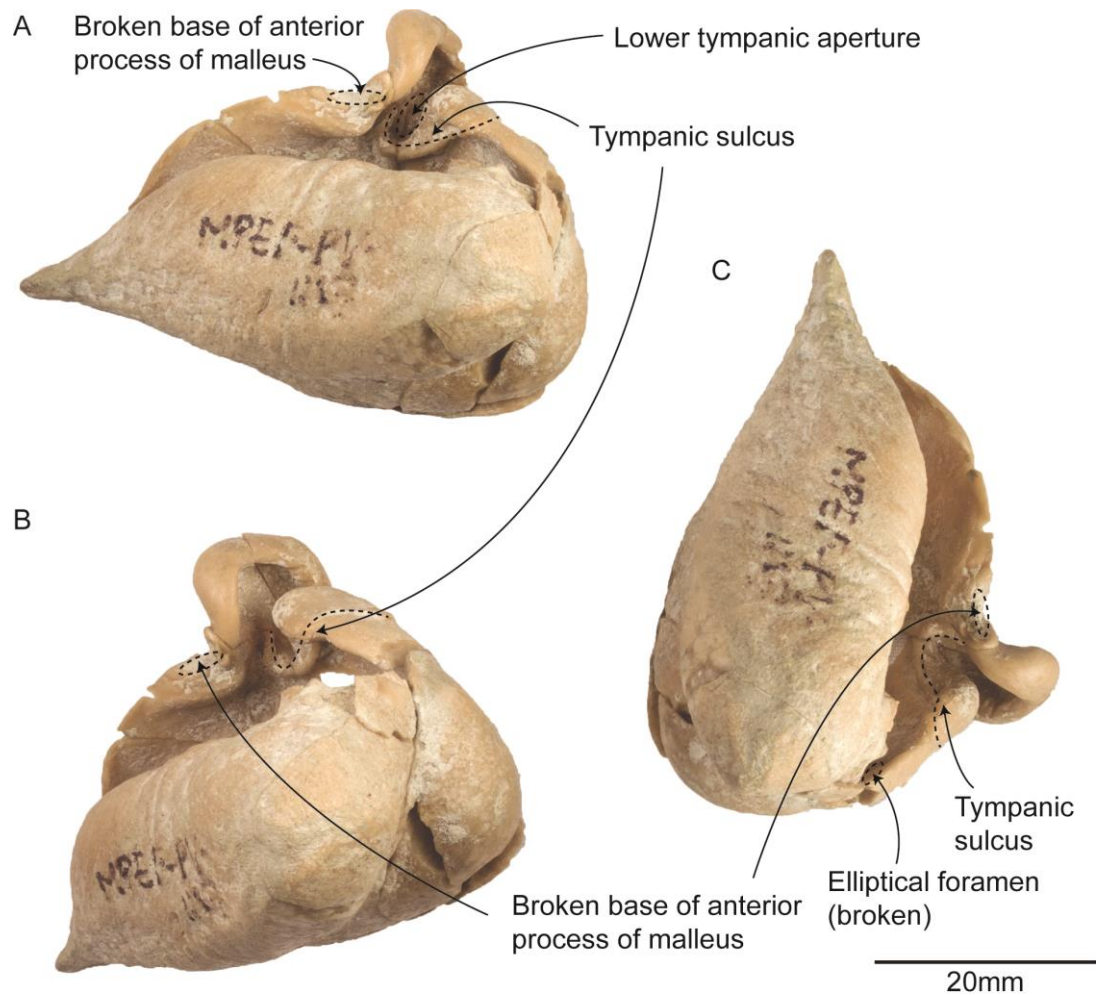


FIGURE S6. Detail of tympanic sulcus in the left tympanic bulla of *Notocetus vanbenedeni* (MPEF-PV 1117). **A**, Posteromedial, **B**, posterior and **C**, medial views.

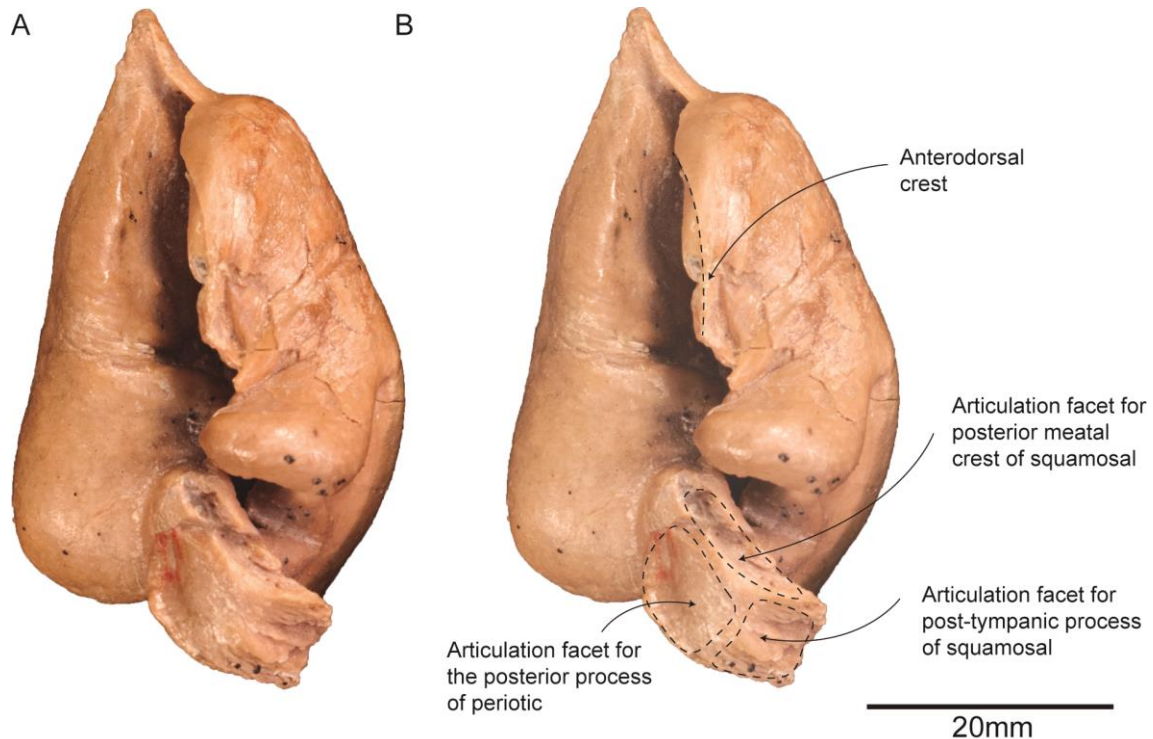


FIGURE S7. Detail of the anterodorsal crest and posterior process in the tympanic bulla of *Notocetus vanbenedeni* (AMNH 29026) in dorsal view **A**, without and **B** with labels.

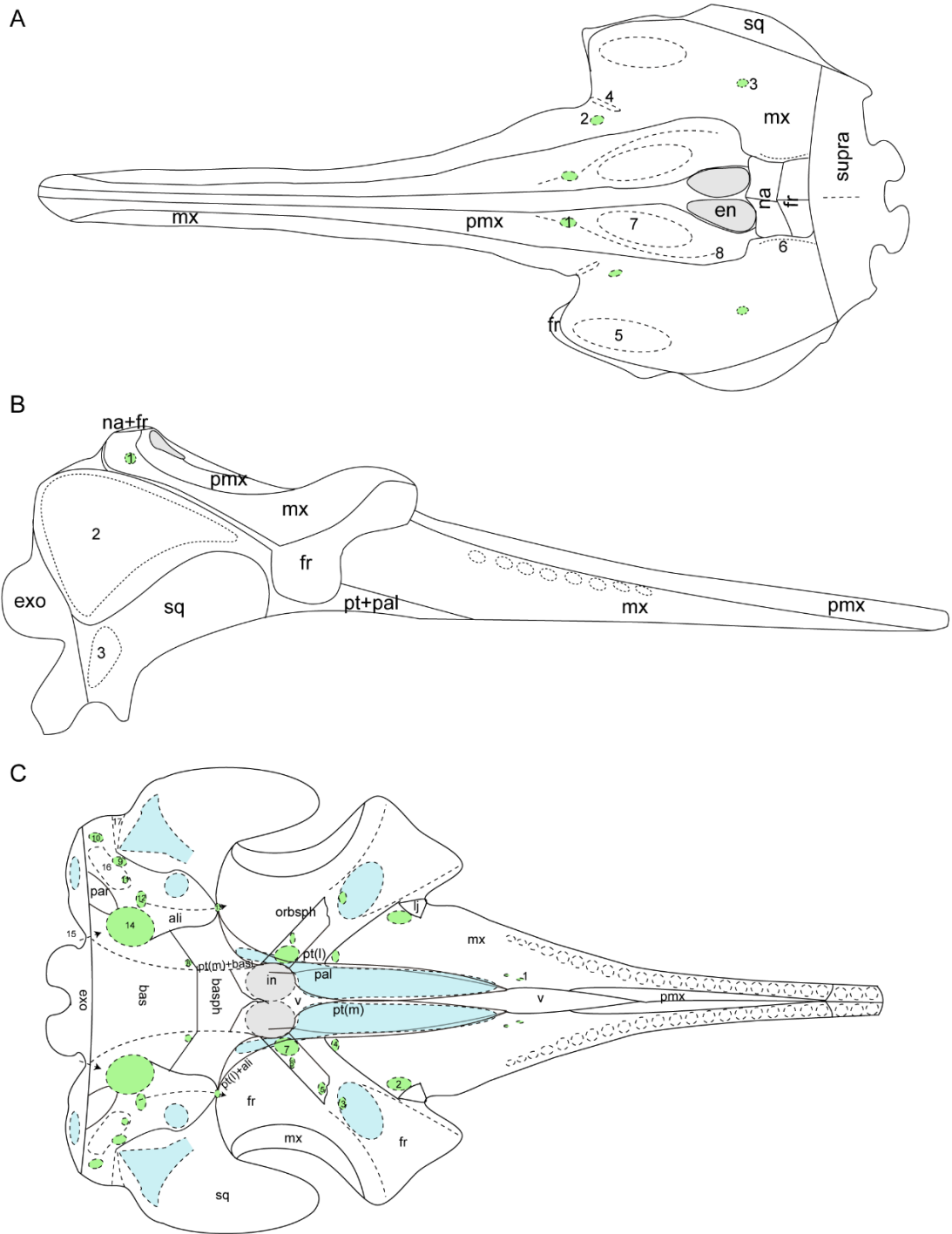


FIGURE S8. Reconstruction of the most important characteristics of the skull of *Notocetus vanbenedeni* in A, dorsal; B, lateral; and C, ventral views, based on all the specimens revised for the present contribution (not to scale). Continuous line indicate sutures, whilst dashed lines indicate structures. Green areas indicate foramen and/or fossa and light blue areas indicate fossae for the pterygoid sinus system. Abbreviations: **ali**, alisphenoid; **bas**, basioccipital; **basph**, basisphenoid; **en**, external nare; **exo**, exoccipital; **fr**, frontal; **in**, internal nare; **lj**, lacrimojugal; **mx**, maxilla; **na**, nasal; **pal**, palatine; **par**, parietal; **pmx**, premaxilla; **pt(m)**, medial lamina of pterygoid; **pt(l)**, lateral lamina of

pterygoid; **supra**, supraoccipital; **sq**, squamosal; **v**, vomer. References: **A**: **1**, premaxillary foramen; **2**, anterior dorsal infraorbital foramen; **3**, posterior dorsal infraorbital foramen; **4**, groove posterior to antorbital notch; **5**, supraorbital crest; **6**, medial facial crest; **7**, premaxillary sac fossa; **8**, posterolateral sulcus; **9**, anteromedial sulcus. **B**: **1**, posterior dorsal infraorbital foramen; **2**, temporal fossa; **3**, neck muscle fossa. **C**: **1**, palatine foramina; **2**, ventral infraorbital foramina; **3**, ethmoid foramen; **4**, sphenopalatine foramen; **5**, optic foramen; **6**, foramen rotundum; **7**, orbital fissure; **8**, ventral carotid foramen; **9**, subcircular fossa; **10**, fossa for the articular rim; **11**, foramen spinosum; **12**, foramen ovale; **13**, external foramen ovale; **14**, cranial hiatus; **15**, jugular notch; **16**, periotic fossa; **17**, externa auditory meatus.

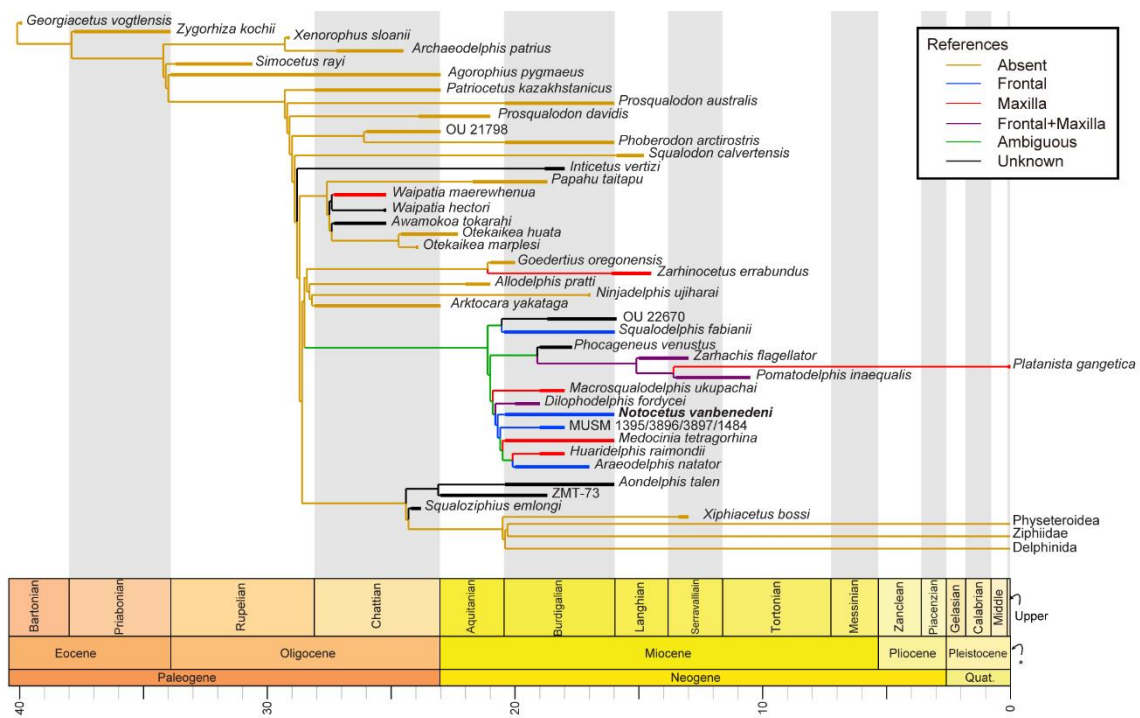


FIGURE S9. Optimization of character “Supraorbital crest, major bones that contributes to it” on the time-calibrated phylogenetic hypothesis obtained under implied weights with K=26. Asterisk indicates the Holocene epoch.

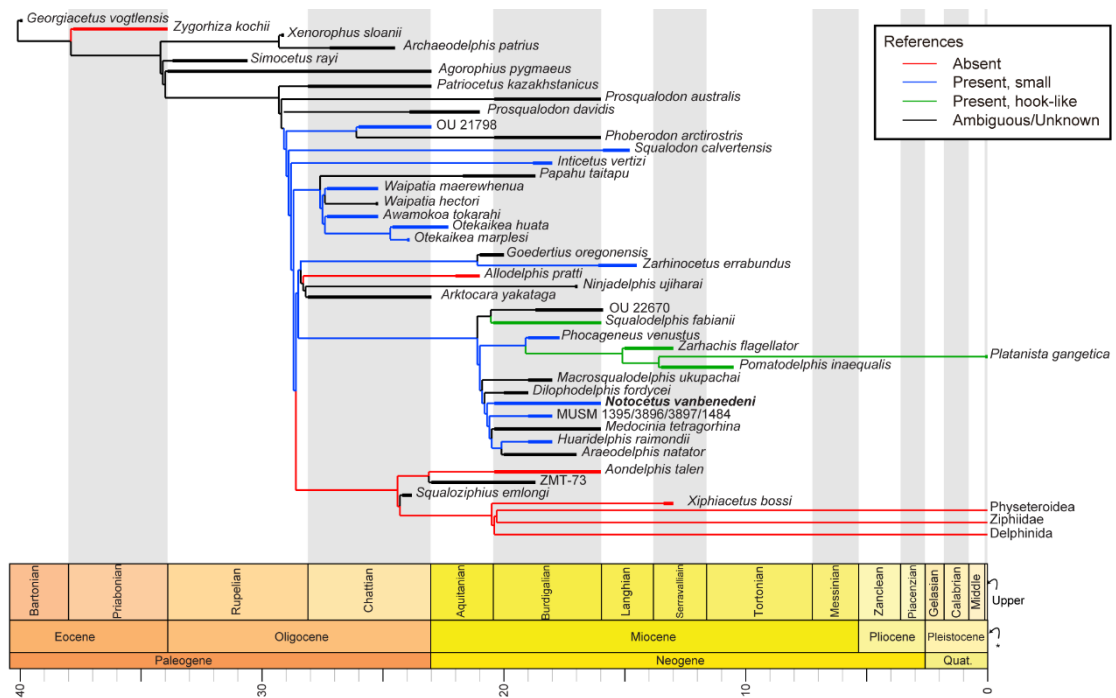


FIGURE S10. Optimization of character “Articular rim of the periotic” on the time-calibrated phylogenetic hypothesis obtained under implied weights with K=26. Asterisk indicates the Holocene epoch.



FIGURE S11. Full strict consensus of 8 MPTs of the phylogenetic analysis under equal weights.

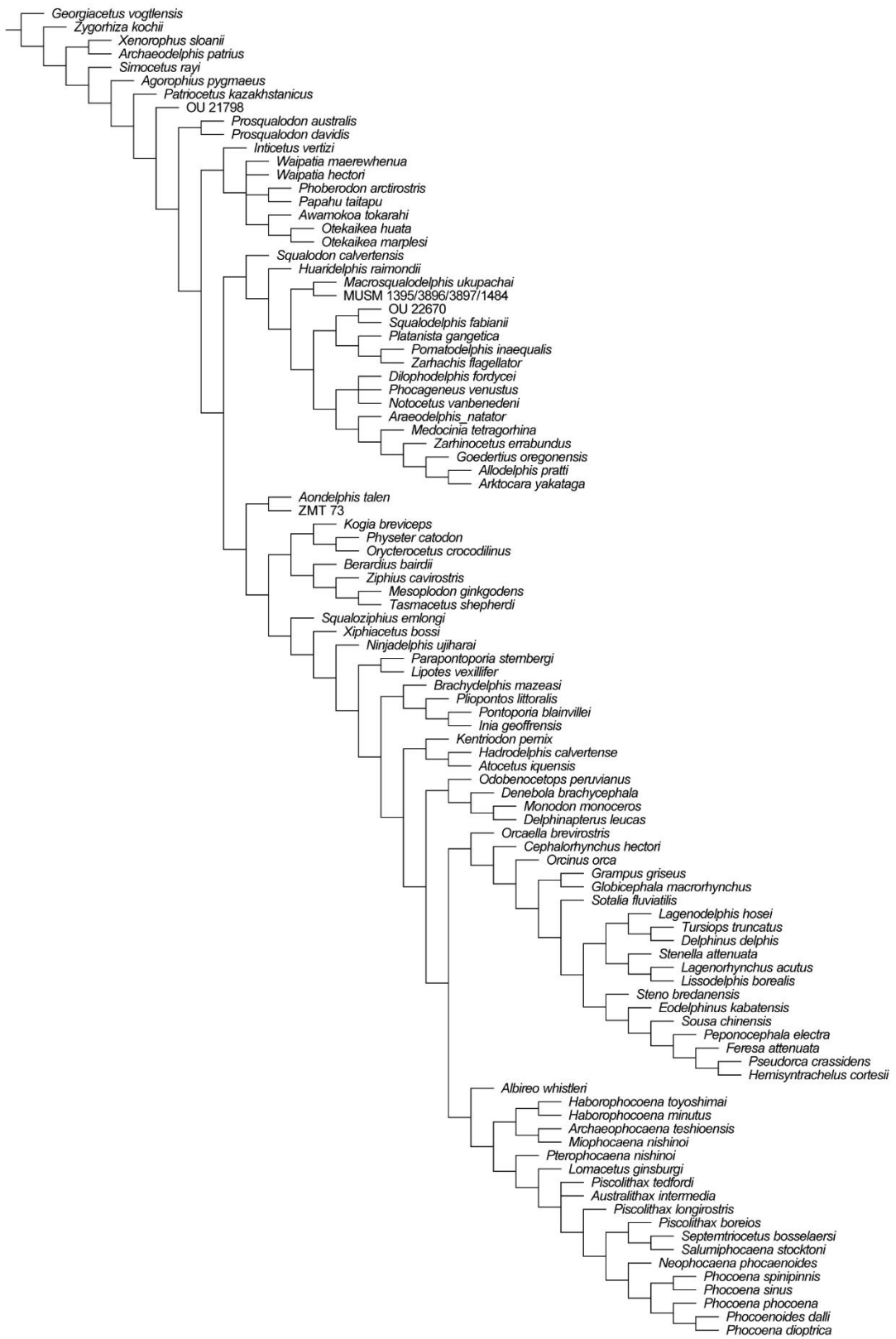


FIGURE S12. Full strict consensus of 2 MPTs of the phylogenetic analysis under implied weights with K=4.



FIGURE S13. Full strict consensus of 2 MPTs of the phylogenetic analysis under implied weights with K=12.



FIGURE S14. Full MPT of the phylogenetic analysis under implied weights with K=16.

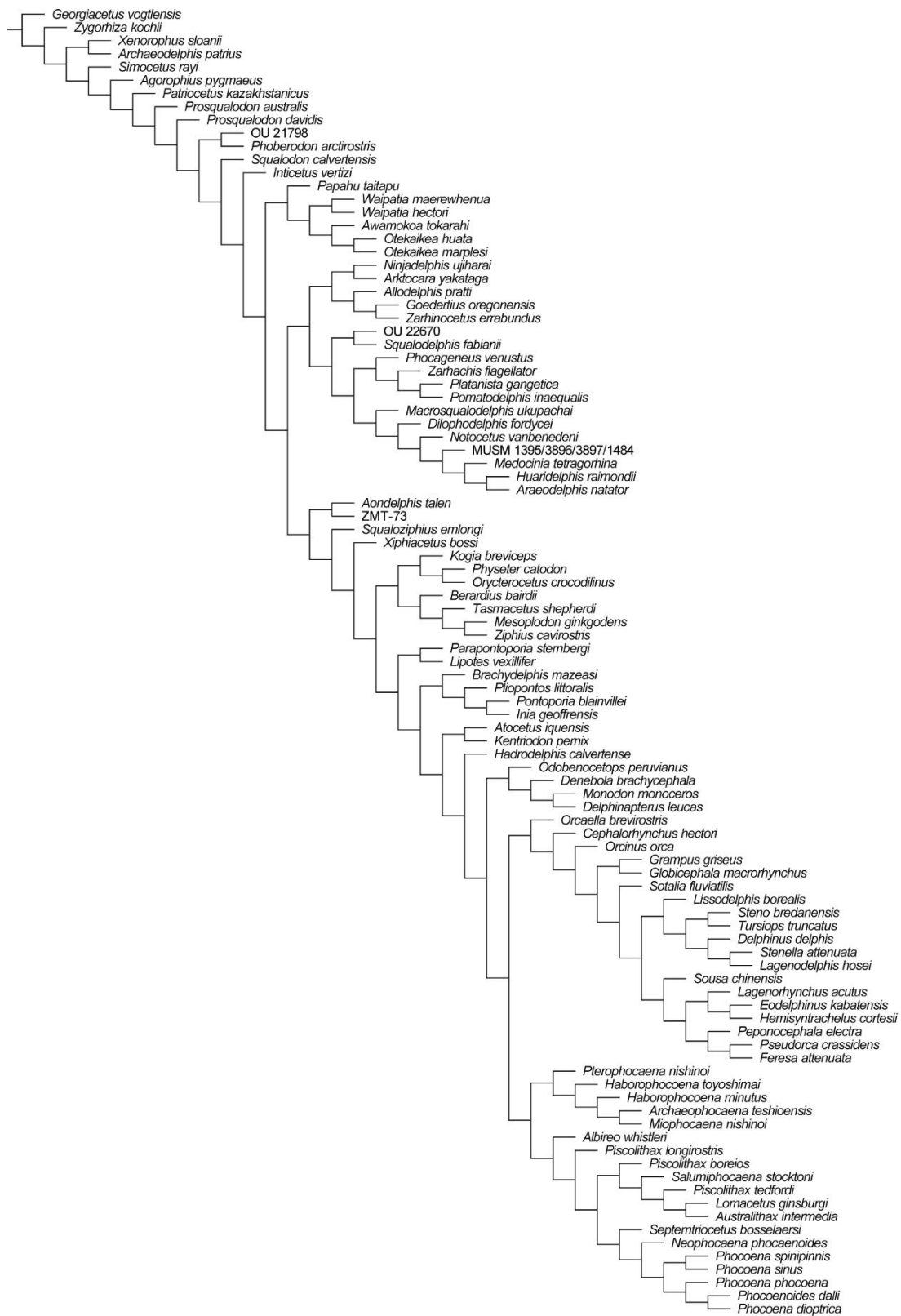


FIGURE S15. Full MPT of the phylogenetic analysis under implied weights with K=18.



FIGURE S16. Full MPT of the phylogenetic analysis under implied weights with

K=26.